RADIATIVE HEAT TRANSFER IN A PARTICIPATING MEDIUM BOUNDED BY DIFFUSELY REFLECTING BOUNDARIES WITH SHORT-PULSE COLLIMATED IRRADIATION.

B N Padhi[a*], P Rath[b], S K Mahapatra[b], A K Satapathy[c]

[a]*Department of Mechanical Engineering*
International Institute of Information Technology,Gothapatana,Bhubaneswar, Odisha-751003, India

[b]*Indian Institute of Technology, Bhubaneswar, Odisha-751 013, India*

[c]*National Institute of Technology, Rourkela,Odisha-769008, India*

* Corresponding Author: Fax: +91.674.3016009 E-mail: biranchipadhi@gmail.com,

ABSTRACT

The transient radiative transfer equation in a two dimensional participating medium bounded by diffusely emitting and reflecting boundaries, one of the boundaries is irradiated with a short pulse laser beam is solved using finite volume method. In the proposed approach, intensity can directly be evaluated by solving the governing transient radiative transfer equation. The effects of optical thickness, scattering albedo and wall emissivity on the transmitted and reflected signals are studied. The performance of two different spatial schemes: STEP and CLAM are also been tested. It is seen that the CLAM scheme gives results to a greater accuracy and hence, correctly predict the speed of photon whereas STEP scheme over predicts the same.

Key words: Transient radiative transfer equation, Participating media, Finite volume method, step, CLAM

Nomenclature

c the speed of radiation intensity
D_c direction cosine
I intensity
$\hat{n}$ the unit outward normal vector
s distance
t time
t_p pulse width
V volume

Greek symbol

β extinction coefficient
θ polar angle
ϕ azimuthal angle
Ω solid angle
τ optical thickness
Φ scattering phase function
σ_s scattering coefficient
ε emissivity
Ψ_T Transmittance
Ψ_R Reflectance

Superscripts

l index for the discrete direction
$*$ non-dimensional quantities
o value from previous time step
~ normalized value

Subscripts

c collimated
D downstream
m modified
P node
P^* value from previous iteration
U upstream
e,w,s,n directions

Introduction

Traditional analysis of radiation transfer neglects the transient effect of light propagation due to the large speed of light compared to the local time and length scales [1]. Of late, with the advent of ultra-short pulsed lasers, this assumption is no longer valid as the temporal width of the input pulse is similar to the order of the radiation propagation time in the system and usually of the order of pico- and femto-seconds. Ultra-short pulsed lasers are used in a wide variety of applications such as thin film property measurements, laser assisted micro-machining, laser removal of contamination particles from surfaces, optical data storage, remote sensing of the atmosphere, combustion chambers, optical ablation and optical tomography [2]. All the applications described above require models to predict transient radiation transport in participating media. In the past, various analytical studies and numerical models of transient radiative transfer have been reviewed by Mitra and Kumar [3].

The commonly used methods to solve the transient radiative transfer equation (RTE) are the Monte Carlo method, the integral equation solution, the finite volume method (FVM), the radiation element method (REM), and the discrete ordinates method (DOM).The Monte Carlo method is often used to simulate problems involving radiative heat transfer because of its simplicity, the ease by which it can be applied to arbitrary configurations and its ability to capture actual and often complex physical conditions [4]. It is computationally time consuming and

demands a lot of computer memory as the histories of the photons have to be stored at every instant of time [4]. Thus, the Monte-Carlo method is ruled out in practical utilizations such as real-time clinical diagnostics where computational efficiency and accuracy are major concerns [5].The backward or reverse Monte Carlo has been developed as an alternative approach, was successfully applied by Lu and Hsu [6] to simulate transient radiative transport in a nonemitting, absorbing, and anisotropically scattering one-dimensional slab subjected to ultra-short light pulse irradiation.

Wu and Coworkers [7, 8] and Tan and Hsu [9] have also used the integral equation formulation to solve the transient radiative transfer problem. Wu [7] used the integral equation to compute the temporal reflectivity and transmissivity of 1-D absorbing and isotropically scattering slabs with various scattering albedos and optical thicknesses which compared well with results obtained using the Monte Carlo method. Tan and Hsu [9] used the formulation to simulate radiative transport in 1-D absorbing and isotropically scattering media with black boundaries exposed to diffuse or collimated irradiation. Finite volume methods developed by Raithby and Chui [10] to solve the steady-state RTE have also been employed to solve the transient RTE by Chai and co-workers [11]. They used the finite volume technique with the ‘‘step’’ and CLAM spatial discretization schemes [11] to model transient radiative transfer in 2-D geometries. Liu et al. [12] and Sakami et al. [13] used the DOM to analyze the ultra-short light pulse propagation in an anisotropically scattering 1-D and 2-D medium. Guo and Kumar [5] used it to simulate short-pulse laser transport in two-dimensional anisotropically scattering turbid media. The discrete transfer method [14], Ray tracing method combined with Hottel's zonal method[15], and a finite element model, which is based on the discrete ordinates method and least-squares variational principle [16] is applied to solve transient radiative transport problems with participating medium. The transport of a train of short-pulse radiation through a 2-D rectangular participating medium with different profiles is examined by R. Muthukumaran, S C. Mishra [17].

Majority of the findings are based on the most simplified assumption of black wall, whereas the reflective wall assumption resembles more to the practical application [3]. Therefore, the present article focuses on the problem of a two dimensional participating medium bounded by diffusely emitting boundaries, under the condition of radiative equilibrium. The total intensity is directly solved using FVM without splitting into the collimated part and diffusive part as cited in existing formulation [14, and 17].

Formulation

A two dimensional rectangular participating medium (Fig.1 a) is considered for the analysis purpose, where the south wall is subjected to square short pulse collimated irradiation (Fig. 1 b). The TRTE for a gray medium can be written as [1]

$$\frac{1}{c}\frac{\partial I(r,\hat{s},t)}{\partial t}+\frac{\partial I(r,\hat{s},t)}{\partial s}=-\beta I(r,\hat{s},t) + k(r)I_b+\frac{\sigma_s(r)}{4\pi}\int_{4\pi} I(r,\hat{s}',t)\phi(r,\hat{s}',\hat{s},t)d\Omega' \quad (1)$$

where the terms on the left hand side represents radiation intensity gradient with respect to time and space. On the right hand side, the first term indicates the attenuation of radiation intensity due to absorption in the direction of travel and out scattering from the direction of travel. The second and third term represent the augmentation part due to emission from the medium and in scattering from all other directions. The discretization equation can be obtained by integrating the TRTE over typical control volume, a control angle and for a small interval of time.For a particular control angle l, the equation (1) can be written as

$$\frac{1}{\beta c}\frac{\partial I^l}{\partial t}+\frac{1}{\beta}\frac{\partial I^l}{\partial s}=-I^l+(1-\omega)I_b + \frac{\omega}{4\pi}\sum_{l'=l}^{M} I^{l'}\Phi^{l'l}\Delta\Omega^{l'} \quad (2)$$

where $I^l = I(r, \hat{s}, t)$ .The inscattering term is summed over all the control angles used to discretize the domain under construction.Now the linearised TRTE can be written as [11]

$$\frac{1}{\beta c}\frac{\partial I^l}{\partial t} + \frac{1}{\beta}\frac{\partial I^l}{\partial s} = -\beta_m^l I^l + S_m^l \tag{3}$$

where modified extinction coefficient,

$$\beta_m^l = \left(1 - \frac{\omega}{4\pi}\Delta\Omega^l\right) - \frac{\omega}{4\pi} a\cos^2\theta^l \Delta\Omega - a\sin^2\theta^l \Delta\Omega^l \tag{4}$$

and modified source function,

$$S_m^l = (1-\omega)I_b + \left\{ \begin{array}{l} \dfrac{\omega}{4\pi}\displaystyle\sum_{\substack{l'=1 \\ l'\neq l}}^{M} I^{l'}\Delta\Omega^{l'} + \\ a\cos\theta \displaystyle\sum_{\substack{l'=1 \\ l'\neq l}}^{M} I^{l'}\cos\theta^{l'}\Delta\Omega^{l'} \\ + a\sin\theta^l \displaystyle\sum_{\substack{l'=1 \\ l'\neq l}}^{M} I^{l'}\sin\theta^{l'}\cos\left(\phi^{l'} - \phi^l\right)\Delta\Omega^{l'} \end{array} \right\} \tag{5}$$

Upon integration over a typical one dimensional control volume and a control angle within a specified time step, the TRTE becomes

$$\begin{aligned} &\int_{\Delta\Omega^l}\int_{\Delta V}\int_{\Delta t^*} \frac{\partial I^l}{\partial t^*} dt^* dv\, d\Omega \\ &+ \frac{1}{\beta}\int_{\Delta\Omega^l}\int_{\Delta V}\int_{\Delta t^*} \frac{\partial I^l}{\partial s} dt^* dv\, d\Omega \\ &= \int_{\Delta\Omega^l}\int_{\Delta V}\int_{\Delta t^*} \left(-\beta_m^l I^l + S_m^l\right) dt^* dv\, d\Omega \end{aligned} \tag{6}$$

Applying divergence theorem to the 2nd term of the equation (6), assuming the magnitude of intensity to be constant over the control volume and a control angle and using the fully implicit scheme, the equation (6) can be written as

$$\begin{aligned} &\left(I_P^l - I_P^{l0}\right)\Delta V\Delta\Omega^l + \frac{1}{\beta}\sum_{i=1}^{4} I_i^l \Delta A_i \Delta t^* \int_{\Delta\Omega^l}(\hat{s}.\hat{n})\, d\Omega \\ &= \left(-\beta_m^l I_P^l + S_m^l\right)\Delta V\Delta\Omega^l \Delta t^* \end{aligned} \tag{7}$$

where I_P^{l0} and I_P^l are the nodal intensities at the start and at the end of the time step respectively. On further simplification, for a control volume and a control angle the equation (7) becomes

$$\begin{aligned} &\frac{\left(I_P^l - I_P^{l0}\right)\Delta V\Delta\Omega^l}{\Delta t^*} + \frac{\left(I_e^l - I_w^l\right)\Delta A_x D_{cx}^l}{\beta} \\ &+ \frac{\left(I_n^l - I_s^l\right)\Delta A_y D_{cy}^l}{\beta} = \left(-\beta_{m,P}^l I_P^l + S_{m,P}^l\right)\Delta V\Delta\Omega^l \end{aligned} \tag{8}$$

where

$$D_{cxe}^l = \int(\hat{s}.\hat{n}_x)d\Omega^l = -D_{cxw}^l$$

$$D_{cyn}^l = \int(\hat{s}.\hat{n}_y)d\Omega^l = -D_{cys}^l$$

$$\Delta\Omega^l = \int_{\Delta\Omega'} d\Omega \qquad \Delta A_x = \Delta A_y \quad \Delta t^* = \beta \times c \times \Delta t$$

To solve the radiative intensity, the boundary intensities are related to the nodal intensities using two different spatial difference schemes namely STEP & CLAM.

Step scheme

In the step or upwind scheme the downstream boundary intensities are set equal to the upstream nodal intensities.

$$I_e^l = I_P^l, I_w^l = I_W^l, I_n^l = I_p^l, I_s^l = I_S^l \tag{9}$$

Applying the STEP scheme, eq (9) becomes,

$$\begin{aligned} &\left[\frac{\Delta A_x D_{cx}^l}{\beta} + \frac{\Delta A_y D_{cy}^l}{\beta} + \beta_{m,P}^l \Delta V\Delta\Omega^l + \frac{\Delta V\Delta\Omega^l}{\Delta t^*}\right] I_P^l \\ &= \left(\frac{\Delta V\Delta\Omega^l}{\Delta t^*}\right) I_P^{l0} + \frac{\Delta A_x D_{cx}^l I_W^l}{\beta} \\ &+ \frac{\Delta A_y D_{cy}^l I_S^l}{\beta} + S_{m,P}^l \Delta V\Delta\Omega^l \end{aligned} \tag{10}$$

So the final discretisation equation for the nodal intensities for the $D_{cx}^{l} \rangle 0$ and $D_{cy}^{l} \rangle 0$ conditions can be written as

$$a_P^l I_P^l = a_P^{l0} I_P^{l0} + a_W^l I_W^l + a_S^l I_S^l + b^l$$

where

$$a_P^{l0} = \frac{\Delta V \Delta \Omega^l}{\Delta t^*}, a_S^l = \frac{\Delta A_y D_{cy}^l}{\beta}, a_w^l = \frac{\Delta A_x D_{cx}^l}{\beta},$$

$$a_P = \left[\frac{\Delta A_x D_{cx}^l}{\beta} + \frac{\Delta A_y D_{cy}^l}{\beta} + \beta_{mP}^l \Delta V \Delta \Omega^l + \frac{\Delta V \Delta \Omega^l}{\Delta t^*} \right]$$

$$b = S_{mP}^l \Delta V \Delta \Omega^l$$

For brevity only STEP scheme is discussed hue to complete the formulation. For details of CLAM scheme, interested readers may refer to [18].

Result discussion

A grid independence test and comparison with available existing solution [13] was done with different spatial and angular grid sizes. It is observed that further refinement to the grid size of 51 × 51 control volumes and 9 × 5 control angles (polar and azimuthal angle) results in negligible change in the results as seen from Fig. 2, where the present method is compared with the DOM used by Sakami et al. [13] with optical thickness as 10, scattering albedo to be 0.998 and non-dimensional pulse width of 1. Although the grid test for non-dimensional time interval sizes is not shown, it is found that the time interval size of 0.01 is producing the optimum results without any significant alteration. Henceforth, the above grid size for space and time is used for further presentation of results.

For all the cases considered, effects are examined with two different spatial differencing schemes such as STEP and CLAM scheme. Figures 3(a, b) represents two particular cases examined to test the performance of both the schemes. It is observed that the CLAM scheme gives more accurate result as compared to the other scheme. Therefore, subsequent results are presented using CLAM scheme.

Figures 4, (a) and (b) shows the influence of anisotropic scattering and wall emissivity on the temporal variation of transmittance and reflectance when the south wall i.e. the wall subjected to collimated radiation becomes grey and all other walls are black. In case of smaller emissivity of wall, the transmittance signal remains for longer time as there is more radiative interaction in the medium because of reflection from the grey south wall. This can be easily observed from the different time rate of decrease of transmittance after the pulse leaves the medium. As seen from the reflectance curve (fig. 4 b), there is a little variation in the peak value. The broadening of curve as the wall emissivity reduces indicates that the signal is relatively significant even after the pulse is switched off. This is due to the effect of the grey south wall and the forward scattering medium. Forward scattering increases the maximum value of the transmitted peaks, whereas there is no significance maximum value of reflectance. The observations from the figures obeys the isotropic scaling rule, which states that forward scattering can be scaled into isotropic scattering with a smaller scattering coefficient and backward scattering can be modeled by isotropic scattering with an increased scattering coefficient.

The effect of wall emissivity on temporal variation of transmittance and reflectance in the presence of anisotropic scattering medium is shown in fig 5, (a) and (b). As seen from fig. 5 (a) the magnitude of transmittance increases with decrease in emissivity of the walls and also the transmittance signal remains for longer time as there is more radiative interaction in the medium as the medium is anisotropically scattering and walls are grey. The rate of decrease of transmittance with time after the pulse leaves the medium gradually reduces as a result of gray walls and forward scattering medium. A different feature is revealed from the reflectance curve (fig. 5 b), as compared to the transmittance graph. There are multiple maxima appeared when the walls are increasingly reflective whereas the secondary maxima vanishes in case of black walls. This is due to the interaction of the gray walls with the anisotropically scattering medium. The back scattered flux gets added to

the reflectance in case of gray wall which causes multiple maxima to appear. The reflected flux reduces as the pulse is switched off and again as a combined effect of the flux reflected from the gray wall and scattered medium flux, the reflected flux creates second maxima.

Figures 6 (a) and (b) presents the influence of optical thickness on transmittance and reflectance when all the boundary walls are gray except the wall subjected to the short pulse collimated radiation. As expected, the magnitude of transmitted flux reduces with increase in the optical thickness. After the pulse left, transmittance signal will tend to leave the medium much faster when the optical thickness of the medium is less. As it is observed from the fig. 6 (b), there are multiple maximas disappearing with higher optical thickness which indicates the dominance of optical thickness over the wall emissivity. The interesting features observed here are that the magnitude of reflectance reduces sharply in case lower optical thickness because higher optical thickness allows radiative interaction in the medium for longer duration.

Conclusion

The transient radiative transfer in a two dimensional participating medium with diffusely reflective boundaries where one of the boundary wall irradiated with a short pulse laser beam is solved. In the proposed approach, one does not have to split the intensity into diffuse and collimated part unlike the case with other existing methods like DTM, DOM, and REM etc. Intensity can directly be evaluated by solving the governing transient radiative transfer equation. The effects of optical thickness, anisotropic scattering, and emissivity of boundary walls on the transmitted and reflected signals are studied. Transmittance decreases with increase in optical thickness. It is to be noted that for a particular optical thickness, as the boundary emissivity decreases, multiple local maxima are appearing in temporal reflectance distribution. The secondary maxima appeared are vanished with the increase in either the optical thickness or the wall emissivity. Moreover, transmittance signal is quite stronger even after the pulse is switched off, when the boundary becomes more gray. The results are examined taking two different spatial schemes: STEP (first order) and CLAM (second order). It is seen that the CLAM scheme gives results to a greater accuracy as compared to STEP scheme.

References

1. Modest, M F, 2002, *Radiative heat transfer*, 2nd edition, CA: Academic Press, San Diego.
2. Kumar, S, Mitra, K, 1999, Microscale aspects of thermal radiation transport and laser applications. Adv Heat Transfer, **33**, pp.187–294.
3. Mitra, K., Kumar, S, 1999, Development and comparison of models for light-pulse transport through scattering absorbing media. Applied Optics **38**, pp.188-196.
4. Guo, Z., Kumar, S, San K-C., 2000, Multidimensional Monte Carlo simulation of short pulse transport in scattering media, Jl. Of Thermophysics Heat Transfer, **14**(4), pp.504-511.
5. Guo, Z., Kumar, S, 2001, Discrete-ordinates solution of short-pulsed laser transport in two-dimensional turbid media, Appl Opt **40**(19), pp.3156–63.
6. Lu, X, Hsu, P-f, 2004, Reverse Monte Carlo method for transient radiative transfer in participating media. ASME Journal of Heat Transfer, **126**, pp. 621-627.
7. Wu, C-Y, 2000, Propagation of scattered radiation in a participating planar medium with pulse irradiation. Journal of Quantitative Spectroscopy & Radiative Transfer, **64**, pp. 537-548.
8. Wu, C-Y, Wu, S-H, 2000, Integral equation formulation for transient radiative transfer in an anisotropically scattering medium. International Journal of Heat and Mass Transfer, **43**, pp. 2009-2020.
9. Tan, Z.M, Hsu, P.F, 2001, An integral formulation of transient radiative transfer. Transaction of ASME, **123**, pp. 466-475.

10. Chui, E. H, Raithby, G. D, 1992, Prediction of Radiative Transfer in Cylindrical Enclosures with the Finite Volume Method, Journal of Thermophysics and Heat transfer, **6** (4), Oct.-Dec.
11. Chai, J.C, 2004, Transient radiative transfer in irregular two dimensional geometries, Journal of Quantitative Spectroscopy and radiative transfer, **84**, pp. 281-294.
12. Liu, L.H.,Ruan, L.M.,Tan, H.P, 2002, On the discrete ordinate method for radiative heat transfer in anisotropically scattering media, International journal of Heat and Mass Transfer, **45**, pp.3259-3262.
13. Sakami, M, Mitra, K, Hsu P F., 2002 Analysis of light-pulse transport through two-dimensional scattering and absorbing media, Journal of Quantitative Spectroscopy & Radiative Transfer, **73**, pp. 169–179.
14. Rath, P, Mishra, S.C, Mahanta P, Saha U.K., Mitra K., 2003, Discrete transfer method applied to transient radiative transfer problems in participating medium, Numerical Heat Transfer Part A: Application, **44**(2), pp.183-197.
15. Tan, H-P, Yi, H-L, 2004, Temperature response in participating media with anisotropic scattering caused by pulsed lasers, Journal of Quantitative Spectroscopy &Radiative Transfer, **87**, pp.175–192.
16. An, W, Ruan, L.M, Tan, H.P, Qi, H, Leo, Y.M, 2007, Finite element simulation for short pulse light radiative transfer in homogeneous and non-homogeneous media, ASME Journal of Heat Transfer, **129**, pp. 353-362.
17. Muthukumaran, R, Mishra, S C, 2008, Thermal signatures of a localized inhomogeneity in a 2-D participating medium subjected to an ultra-fast step-pulse laser wave, Journal of Quantitative Spectroscopy &Radiative Transfer, **109**, pp.705–726.
18. Coelho P.J, 2002, Bounded skew high order resolution schemes for the discrete ordinates method, Journal of Computational physics, **175**, pp.412-437.

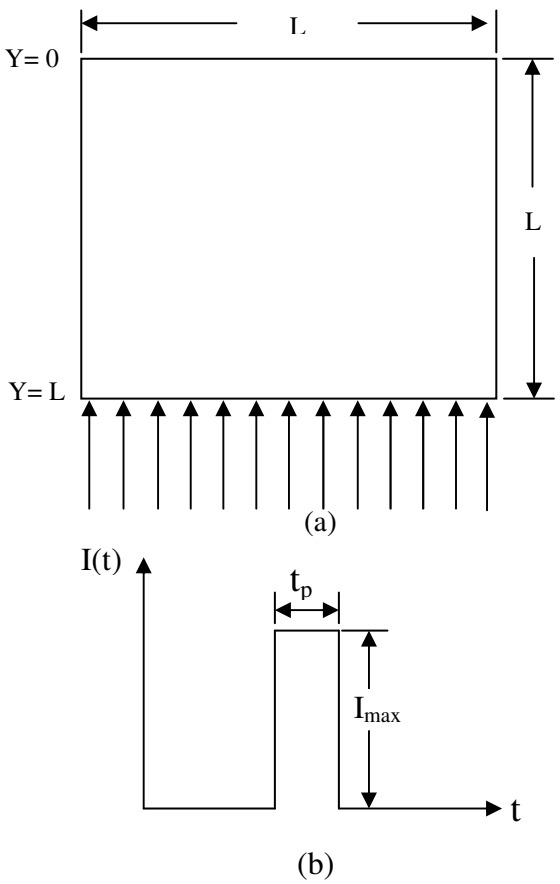

Fig.1 (a) Computational domain, (b) square pulse

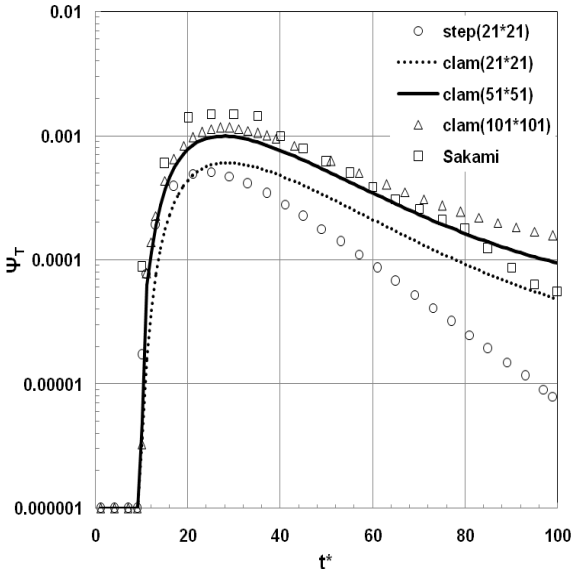

Fig.2 Grid Independence test,

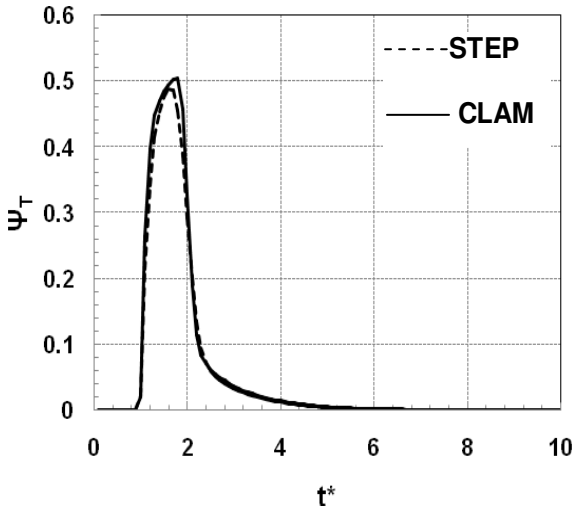

(a)

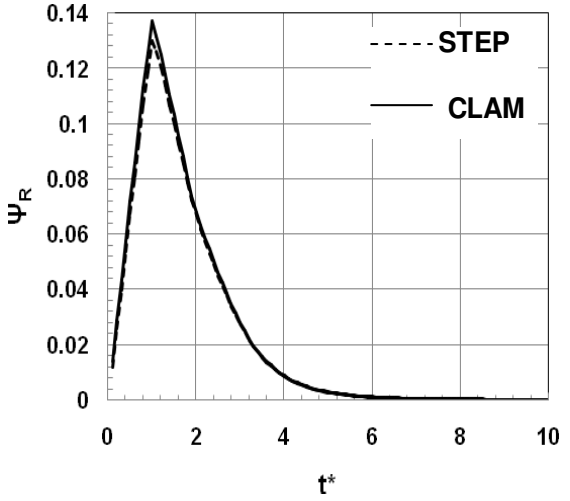

(b)

Fig. 3 Performance of step and clam scheme.(a) Transmittance, (b) Reflectance with $\tau = 1.0$,a = 0.9, $\omega = 1.0$, $\varepsilon_S = 0.25$

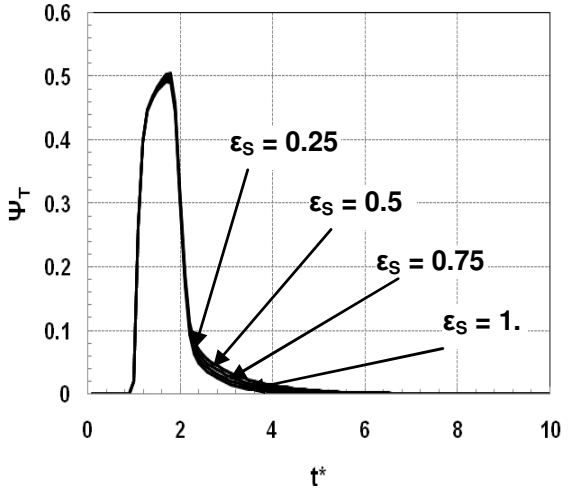

(a)

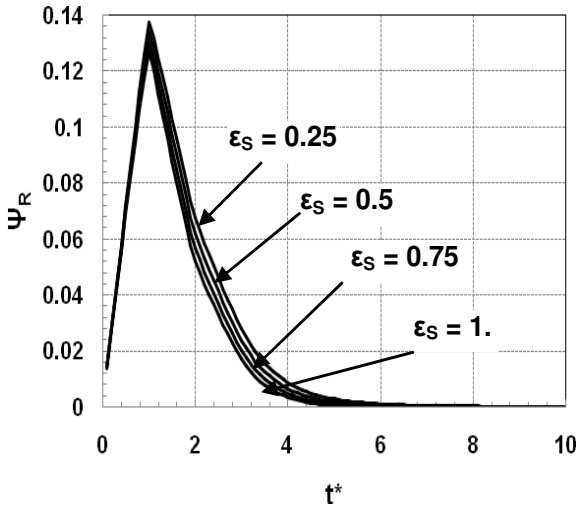

(b)

Fig. 4 Effect of grey south wall and other black walls on (a) Transmittance and (b) Reflectance for with $\tau = 1.0$, a = 0.9, $\omega = 1.0$.

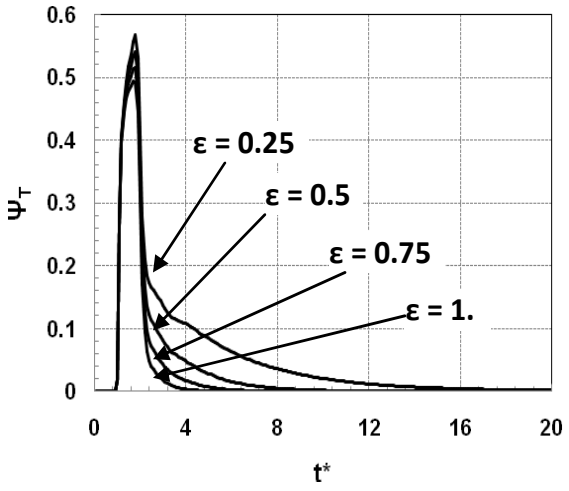

(a)

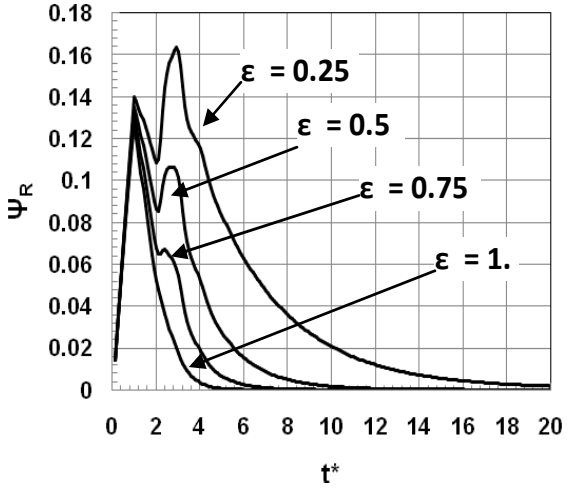

(b)

Fig.5 Effect of all grey walls on (a) Transmittance and (b) Reflectance for $\tau = 1.0$, a = 0.9, $\omega = 1.0$

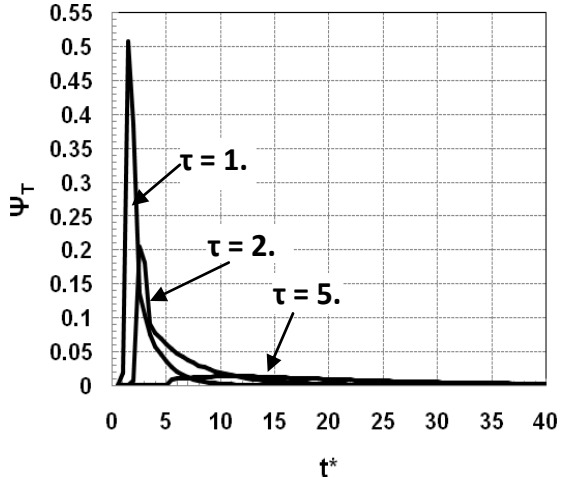

(a)

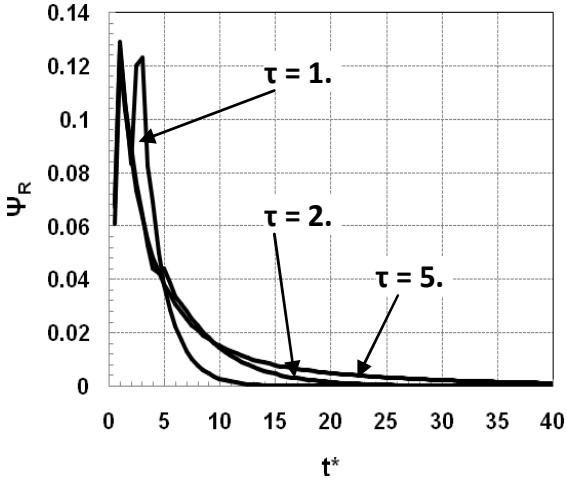

(b)

Fig. 6 Effect of optical thickness on (a) Transmittance and (b) Reflectance for a = 0.0, $\varepsilon_e = \varepsilon_w = \varepsilon_n = 0.25$, $\varepsilon_s = 1.0$ and $\omega = 1.0$